



Mössbauer study of exogenous iron redistribution between the brain and the liver after administration of $^{57}\text{Fe}_3\text{O}_4$ ferrofluid in the ventricle of the rat brain



Dmitry Polikarpov^{a,d,*}, Raul Gabbasov^a, Valery Cherepanov^a, Natalia Loginova^b, Elena Loseva^b, Maxim Nikitin^c, Anton Yurenia^{a,e}, Vladislav Panchenko^{a,e}

^a National Research Center "Kurchatov Institute", Moscow, Russia

^b Institute of Higher Nervous Activity and Neurophysiology, Russian Academy of Sciences, Moscow, Russia

^c Shemyakin-Ovchinnikov Institute of Bioorganic Chemistry, Russian Academy of Sciences, Moscow, Russia

^d Russian National Research Medical University named after N.I.Pirogov, Moscow, Russia

^e Lomonosov Moscow State University, Moscow, Russia

ARTICLE INFO

Article history:

Received 29 June 2014

Received in revised form

19 October 2014

Available online 22 October 2014

ABSTRACT

Iron clearance pathways after the injection of $^{57}\text{Fe}_3\text{O}_4$ -based ferrofluid into the brain ventricles were studied histologically and by Mössbauer spectroscopy. It was found that the dextran coated initial nanobeads of the ferrofluid disintegrated in the brain into separate superparamagnetic nanoparticles within a week after the injection. The exogenous iron completely exited all ventricular cavities of the brain within a week after the injection but remained in the white matter for months. Kupffer cells with the exogenous iron appeared in the rat liver 2 hours after the injection. Their concentration reached its maximum on the third day and dropped to zero within a week. The exogenous iron appeared in the spleen a week after the injection and remained in the spleen for months.

© 2015 Elsevier B.V. All rights reserved.

1. Introduction

Methods of a medication treatment of brain diseases are principally different from the methods of treatment of other human organs due to the presence of the skull. The braincase prevents direct injection of the drug to the pathological region of the brain by the syringe. Another traditional method of drug delivery is its delivery through the blood circulation by immersing the drug into the bloodstream. This method also proves to be ineffective too due to the presence of the blood–brain barrier (BBB)—a system of endothelial cells that separates the blood from other intrabrain fluids—interstitial fluid bathing neurons and neuroglia and the cerebrospinal fluid that circulates around brain ventricles and spinal cord [1]. As a result, nearly 98% of exogenous molecules passing through the blood vessels in the brain do not cross the blood vessel walls [2]. That's why the drug delivery through the BBB is a challenge in the treatment of brain's oncological or neurological disorders. Various strategies have been proposed to circumvent the BBB. The simplest transcranial approach invasively bypasses the BBB by drilling a hole in the skull and injecting

probes or drugs intracerebrally or intracerebroventricularly [3]. At present, intracerebral injection is the gold standard in the field, however the procedure of opening the skull is very dangerous [4,5]. Colloidal magnetic drugs show great promise as drug delivery systems for alternative passing through the BBB. The technology is based on the concentration of the magnetic drug in the blood vessels of the brain by external magnetic field [6–9]. This is followed by the transportation of the drug through the barrier which is performed using monocytes/macrophage [10–15], ultrasonic [16,17] or optical [2] methods. Usually the magnetic beads for in vivo application consist of superparamagnetic nanoparticles of iron oxide. The choice of the iron is due to the assumption of its biocompatibility: human organism contains about 4 g of endogenous iron, mainly in ferritin and hemoglobin forms. On the other hand, the nanoparticles exhibit higher toxicity as compared to the molecular form, can penetrate through the cell barriers, circulate and accumulate in organs and tissues. The specific feature of the brain, which is the presence of the blood–brain barrier, additionally complicates the processes of clearance of nanoparticles. Therefore, the question of whether there is a mechanism of biodegradation or excretion of iron nanoparticles from the brain is crucial for the development of the described technology, and requires a clear answer for the introduction of the method into clinical practice. In [18] we used a direct transcranial injection

* Corresponding author at: National Research Center "Kurchatov Institute", Moscow, Russia.

E-mail address: polikarpov.imp@gmail.com (D. Polikarpov).

procedure in order to bypass the blood–brain barrier. There is no barrier between the interstitial and the cerebrospinal fluid. As a result, the nanoparticles staying in either of these two fluid compartments are free to exchange and reach any brain structures [2,19]. Three months later the brain was extracted and analyzed with the histological and Mössbauer spectroscopy methods. It was found that Fe_3O_4 nanoparticles had completely disappeared from the brain. Unfortunately, within the framework of our preliminary study we were not able to determine the mechanism of particles excretion. This excretion may be caused both by biodegradation in the brain and excretion from the brain followed by subsequent biodegradation in the liver. In the present study we tried to elucidate this mechanism.

1.1. Experimental

1.1.1. Magnetic particles

$^{57}\text{Fe}_3\text{O}_4$ magnetic nanoparticles were synthesized by co-precipitation of water solution of hydrate of iron chloride $\text{FeCl}_2 \cdot 4\text{H}_2\text{O}$ and solution of $^{57}\text{FeCl}_3$ in 0.1 M HCl ($\text{Fe}^{2+}:\text{Fe}^{3+} = 1:2$) in 30% solution of ammonium hydroxide, NH_4OH . After incubation at 90 °C,

the particles underwent magnetic separation and flushing in 2 M HNO_3 followed by their introduction into distilled H_2O to form a suspension. The as-produced suspension was supplemented with 70 kDa dextran from *Leuconostoc* spp. (Sigma, USA). After re-incubation at 80 °C, the particles were triply flushed in dH_2O by centrifuging. Then the particles were sorted for the selection of batches of particles with similar dimensions. The powder of $\alpha\text{-}^{57}\text{Fe}_2\text{O}_3$ enriched to not less than 99% by stable isotope ^{57}Fe used in this work was obtained from JSC “PA “Electrochemical Plant”, Russia. The initial trivalent $^{57}\text{FeCl}_3$ was synthesized by direct solving $\alpha\text{-}^{57}\text{Fe}_2\text{O}_3$ in HCl. As a result the as-produced $^{57}\text{Fe}_3\text{O}_4$ nanoparticles are enriched in the ^{57}Fe stable isotope minimum to 66%, which is more than 30-fold excess of the ^{57}Fe content in nanoparticles of magnetite of natural isotope composition [20].

1.1.2. Rats

17 Wistar rats weighting 200–250 g were used for the experiment. The animal care facility was kept under a natural light/dark cycle. The rats were housed individually and were provided with water and food ad libitum. All animal care standards and protocols were in compliance with the NIH guide for the care and use of

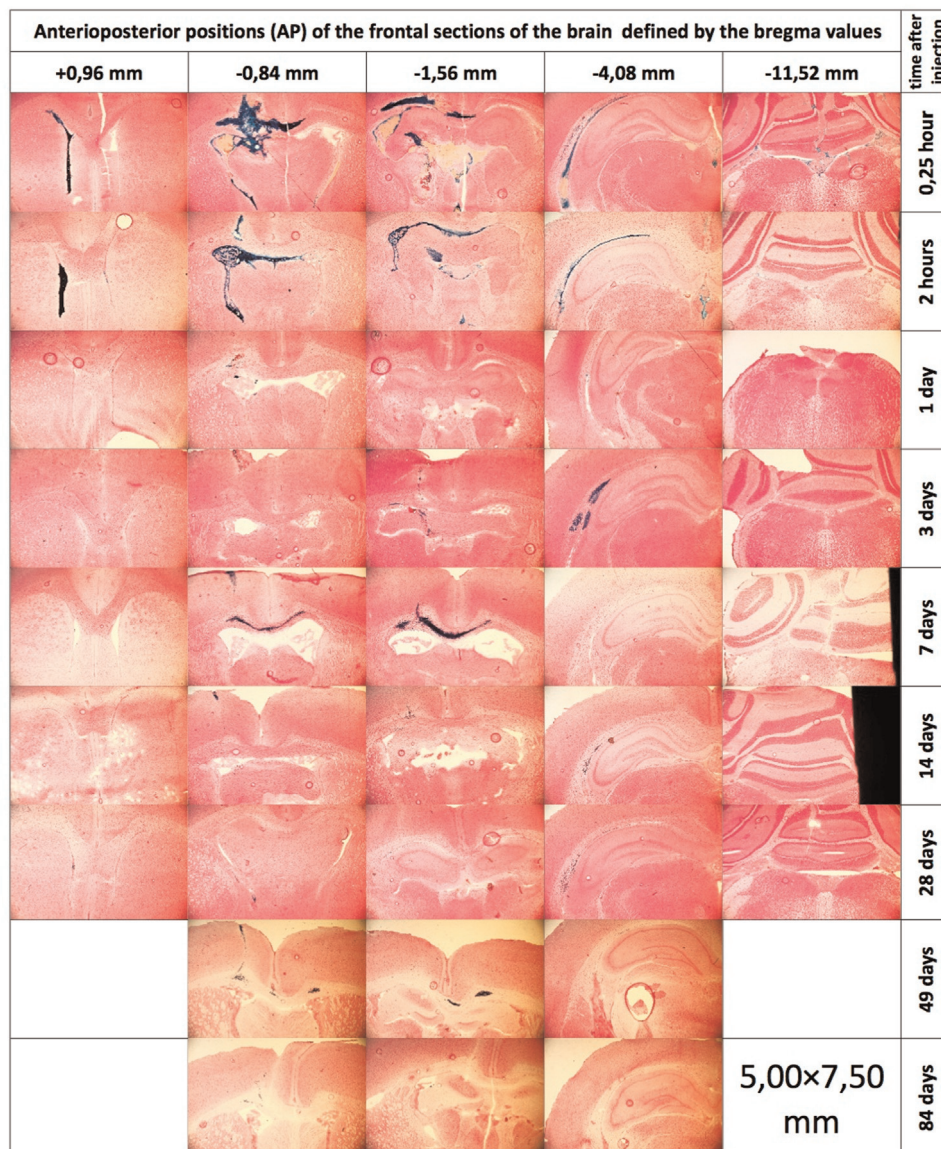


Fig. 1. Cross-sections of rat brains at different depths are shown at different time points after the injection of ferrofluid, stained on ferric iron (Prussian blue).

laboratory animals (NIH Publications no. 80-23, revised 1996). Five milligrams of the magnetic nanoparticles (dry weight of iron oxide) suspended in 5 μL of PBS were injected transcranially in the right lateral ventricle of the brain (AP = -0.8 mm, L = 1.5 mm, H = 3.8 mm, according to atlas [21]). The injections were performed under chloral hydrate anesthesia (400 mg/kg). The rats were sacrificed in 15 min, 2 h, 1, 3, 7, 14, 28, 49 and 84 days after the injection. Brain, liver and spleen were extracted for morphological and Mössbauer studies.

1.1.3. Methods

1.1.3.1. Histology. The main aim of the presented study was to see a transfer of iron from exogenous nanoparticles to any endogenous form of iron. There are many endogenous iron phases in the brain tissue, which include heme iron, different forms of ferritin and hemosiderine, magnetite, maghemite and even wustite [22–28]. The first histochemical study of the iron concentration distribution in the brain was fulfilled by Spatz [29] almost one hundred years ago using Perl's staining method. Since then, the method has become a major in the study of iron distribution despite the

variety of possible forms of iron in the brain, noted above. In reality the Perl's staining is selectively sensitive to the ferric iron. So it cannot be equally sensitive to all forms of brain iron. For example, iron revealed by Perl's stain usually has a higher concentration in the grey matter, with negligible staining in the white matter. However recent magnetic resonance imaging studies revealed that iron concentrations in some white matter regions are similar to those in grey [30]. Generally the valence state of iron can switch between ferric (Fe^{3+}) and ferrous (Fe^{2+}) under in-vivo conditions in the processes of iron uptake, transport, and storage [31]. Therefore, in this work we tried both ferric (Perls) and ferrous staining.

1.1.3.1.1. Sampling. Sampling of material for histological studies was performed using perfusion. For this purpose the animals were anesthetized with Nembutal (50 mg/kg). Through the circulatory system of the rat passed the first wash solution for 2 min containing 0.9% sodium chloride solution with 0.02% sodium heparin, and then the first fixing solution (2% solution of paraformaldehyde in phosphate buffer, pH = 7.2 – 7.4), for 3 min and the second fixing solution (4% paraformaldehyde solution in phosphate buffer,

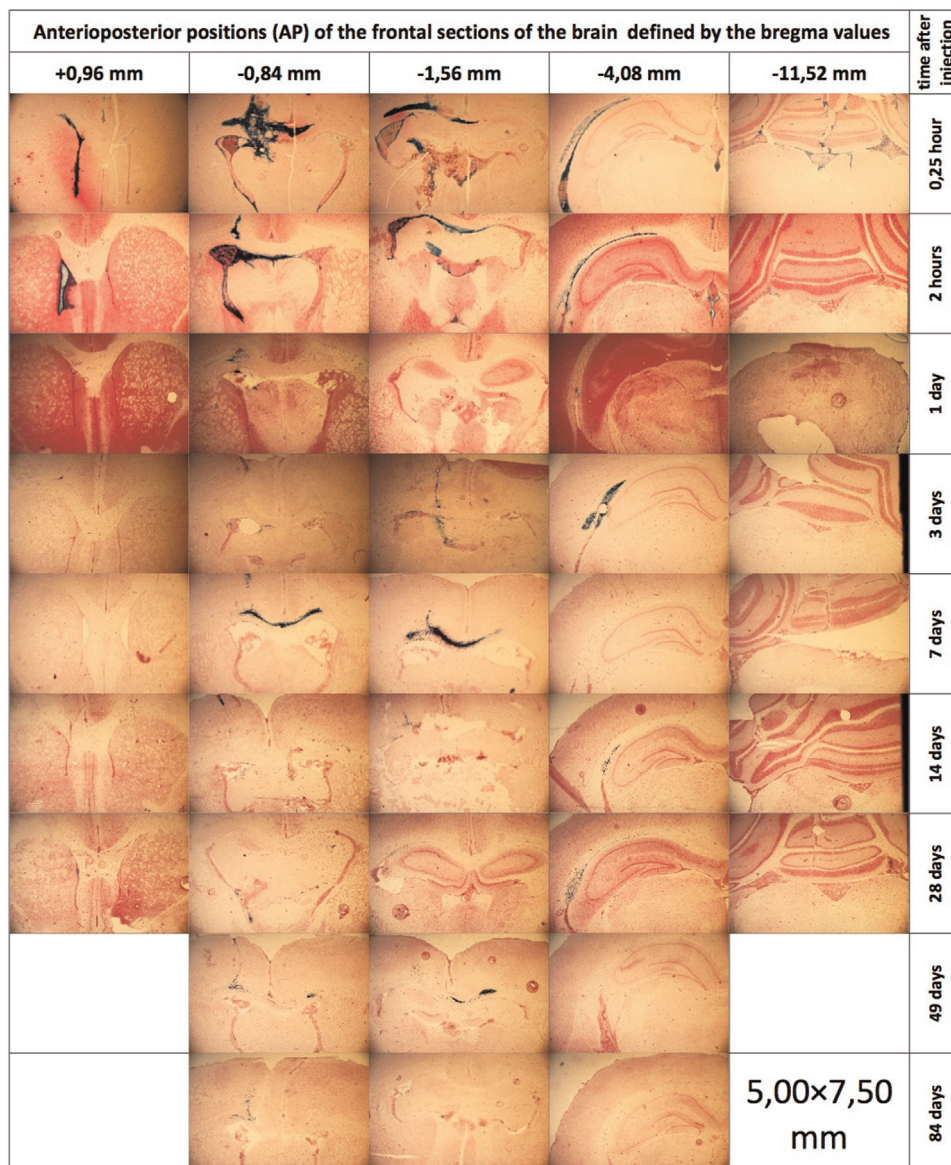


Fig. 2. Cross-sections of rat brains at different depths are shown at different time points after the injection of ferrofluid, stained on ferrous iron.

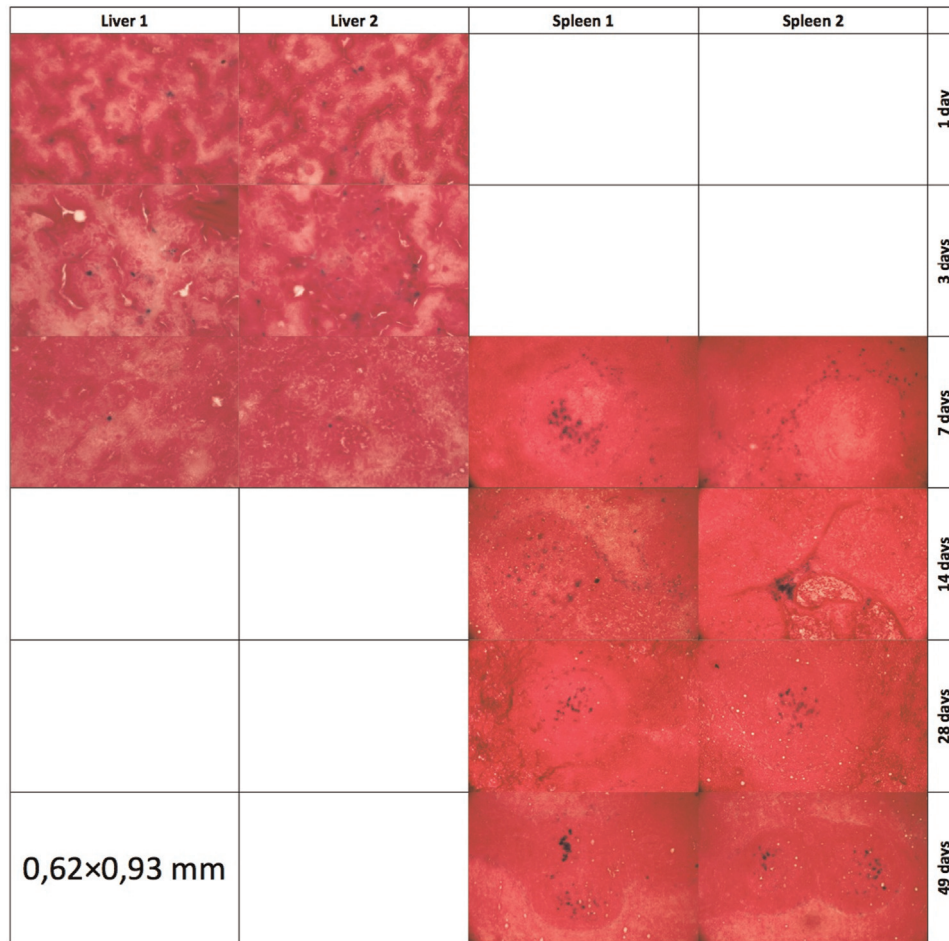


Fig. 3. Cross-sections of the liver (two random samples) and the spleen (two random samples) of the rats are shown at different time points after the injection, stained on ferric iron (Prussian blue).

pH=7.2–7.4), for 10 min. Then the brain, liver and spleen were extracted and placed in 4% paraformaldehyde solution in phosphate buffer (pH=7.2–7.4). For histological studies the organs for 12 h were placed in 20% sucrose solution in phosphate buffer pH=7.2–7.4) at a temperature of 40 °C. Then they were dried by filter paper and frozen in liquid nitrogen vapor. The slices thick 18 μ m were produced on a cryostat Zeiss Microm HM 505 E at a temperature of -20 °C to 22 °C. In the brain we did 5 sections: +0.96 mm, -0.84 mm, -1.56 mm, -4.08 mm, -11.52 m to bregma. In the liver we did 3–4 sections of 3 liver lobe. The resulting sections were mounted on glass slides Menzel GmbH&Co KG, coated with a solution of gelatin. The resulting slices were dried at room temperature for 24 h.

1.1.3.1.2. Stain on ferric iron (Perls stain). Portion of sections were stained by the Perls (the reaction product—Prussian blue). To do so, we first prepared staining solution containing 2% aqueous solution of potassium ferrocyanide and 2% solution of hydrochloric acid, which were mixed together in equal proportions immediately before use. Staining was performed as follows: the dye was applied to the slices for 30 min, then the glass slides with slices were put in 70% (30 s), 96% (30 s), and twice in 100% (30 s) alcohol, and then 2 min the glass slides with slices were placed in toluene. Slices were entered in the medium (Bio Optica, Italy) under a coverslip. Stained slices were examined under a light microscope Axioplan 2 (Zeiss, Germany). As a result of the staining clusters of Fe_3O_4 nanoparticles and clusters of hemosiderin in macrophages become dark blue, cell nuclei, basophilic substance and fibrin acquire different shades of red.

1.1.3.1.3. Stain on ferrous iron. Staining of sections was performed for 1 h in a freshly prepared solution of 0.4 g of potassium ferricyanide in 40 ml of an aqueous solution of hydrochloric acid (2.5 mL of hydrochloric acid and 497.5 mL of distilled water). The slices were then washed in 1% acetic acid (1 mL glacial acetic acid and 100 ml of distilled water). After rinsing in distilled water, sections were stained with the dye in Nuclear Fast Red Sodium Salt for 5 min. After rinsing in distilled water, sections were dehydrated in alcohols of increasing concentration: 70°, 96°, 100°. The sections were then placed for 5 min in toluene and embedded in the medium (Bio Optica, Italy) under the coverslip. As a result of the staining a ferrous iron becomes blue.

1.1.3.2. Mössbauer spectroscopy. The lyophilized tissue were ground for preparation of the samples for Mössbauer study. The Mössbauer absorption spectra of ^{57}Fe nuclei in the prepared samples were measured at room temperature on a conventional spectrometer in the constant-acceleration regime and transmission geometry using a $^{57}\text{Co}/(\text{Rh})$ radioactive source.

2. Results and discussion

2.1. A. Histological examination

2.1.1. Study of the brain

It is known that the magnetic beads rapidly change their physical and chemical properties after administration into a living

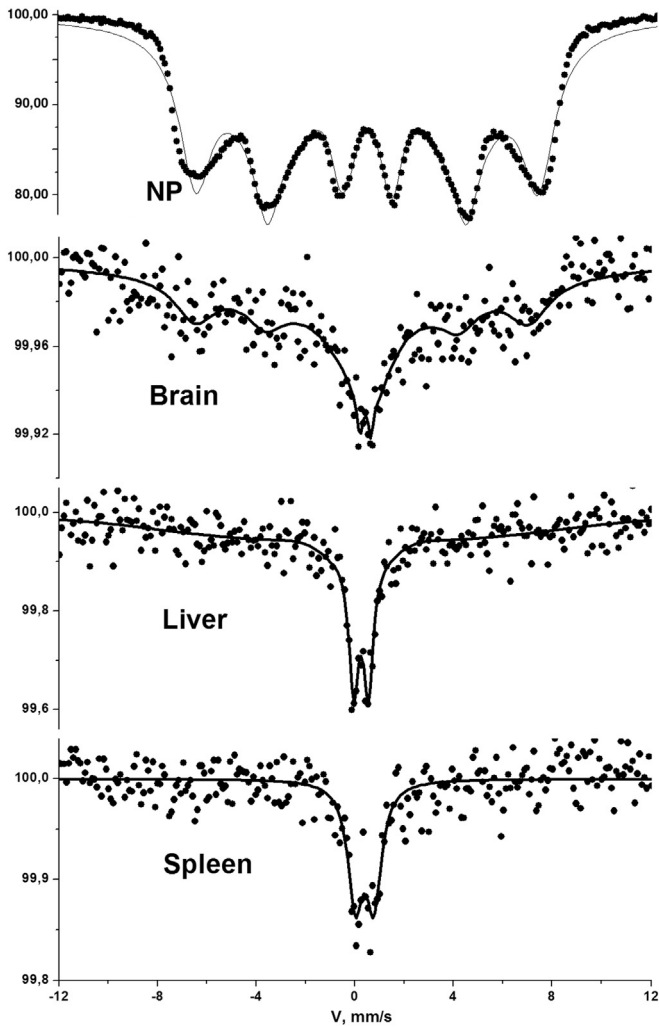


Fig. 4. ^{57}Fe Mössbauer spectra of intrinsic $^{57}\text{Fe}_3\text{O}_4$ nanoparticles (NP), brain, liver and spleen, measured 1 day after the injection. $T=300$ K.

organism [32]. Therefore, the coloring of brain sections was done by the dyes, selective to the trivalent iron (Fig. 1) and to the divalent iron (Fig. 2). It was done in order to identify any possible products of their disintegration and biodegradation. 15 min and 2 h after administration of the ferrofluid into the left lateral ventricle, 2- and 3-valent iron was detected at all levels of the brain ventricles till cerebellum, and in some areas of white matter in the left cerebral hemisphere. Iron in a small amount was also detected in the ventricle of the right hemisphere. After 3 days, the iron remains in the left ventricle (levels 2–4) and white matter (levels 3–4). After 7 days, the iron in a very small amount was observed in the lateral ventricle. The content of iron in the white matter in both hemispheres at 2–3 levels remained as high. After 14 days the individual granules of iron were found in the loops of the choroid plexus in the ventricles and the bit in the white matter at levels of 1–4 (2-valent iron) or 2–4 (3-valent iron). After 28 days the iron was found only in the white matter. Everywhere the content of divalent iron is more than trivalent. After 49 days the iron remained only in the white matter of both hemispheres at levels 2 and 3. In ventricular cavity iron was absent. We saw only solitary individual granules in the loops plexus. After 84 days the iron was found only on the 2 and 3 levels in the white matter of the left hemisphere.

To summarize we can conclude that ferrous and ferric iron were found in the brain in all days after injection. The greatest amount was detected immediately after injection, the lowest—49 and 84 days. After 7 days the iron was not determined in the ventricular cavities, except for rare content in the loops of the choroid plexus. However, the iron still remains in the white matter. Iron that has reached the white matter will stay there for very long time periods.

2.1.2. Study of the liver and the spleen

Fig. 3 shows the cross-sections of the liver (two random samples) and the spleen (two random samples) of the rats 1, 3, 7, 14, 28 and 49 days after the injection of ferrofluid, stained on ferric iron (Prussian blue). In the liver both 2 and 3 valent iron was found only in the early period after administration of the ferrofluid into the lateral ventricle of the brain. Iron containing macrophages (Kupffer cells) were seen already after 2 h. The number of such cells was increased within 24 h. After 3 days the number of such cells was maximum. After 7 days the iron was not detected in the liver. It is seen that, unlike the clearing of liver, the clearing of the spleen occurs heavily, so the iron was stored in it during all the periods of the experiment.

2.2. Mössbauer Spectroscopy

Histochemical method enables to see the picture of iron spatial distribution on the slices of the rat's organs. Unfortunately, this method cannot give information about the physical and chemical state of the iron. On the contrary the Mössbauer spectroscopy method is insensitive to the spatial distribution of the iron but is able to distinguish magnetic nanoparticles with different sizes or the iron in different chemical compounds. Fig. 4 shows the ^{57}Fe Mössbauer spectra of intrinsic $^{57}\text{Fe}_3\text{O}_4$ nanoparticles (NP) in comparison with the spectra of the brain, liver and spleen, measured one day after injection of this NP. It is seen that the inclusions of the exogenous iron in these organs, which looked the

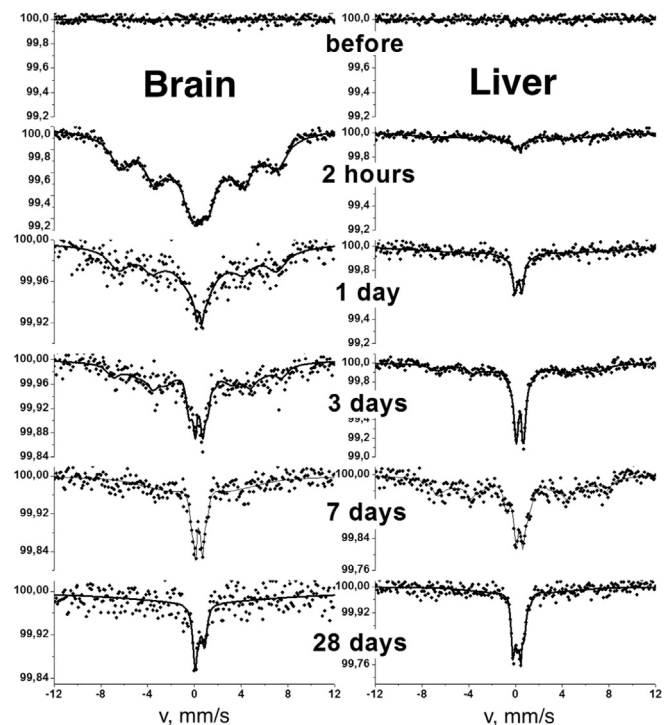


Fig. 5. ^{57}Fe Mössbauer spectra of brain and liver, measured before injection, 2 h, 1, 3, 7, 28 days after the injection. $T=300$ K.

same on the histological Figs. 1, 2 and 3, are characterized by different Mössbauer spectra.

Mössbauer spectrum of the intrinsic magnetic nanoparticles in Fig. 4 represents a Zeeman sextet of lines. The asymmetrical shape of its lines with sharp outer and smeared inward sides gives evidence of the presence in the sample of the ensemble of superparamagnetic nanoparticles, which are connected by magnetic dipole interactions. The spectrum of these particles in the brain is completely different and characterized by the presence of Zeeman sextet of lines superimposed on the very broad central doublet of lines. Extreme width of the doublet indicates its relaxation nature, i.e., it reveals the presence in the sample of the oscillations of the magnetization vectors with a frequency commensurate with the lifetime of the excited state of the Mossbauer nucleus (10^{-8} s). Spectrum of magnetic nanoparticles in the liver is characterized by the presence of a much weaker Zeeman sextet of lines superimposed on the sharp central doublet of lines. This shape of the spectrum indicates the presence in “1 day” liver of smaller magnetic clusters and much smaller sized nanoparticles than in the “1 day” brain. The “1 day” spectrum of the spleen reveals an absence of the interparticle dipole magnetic interaction in the sample at all.

Mössbauer spectra of the liver and the brain measured in different time intervals after the transcranial injection of the magnetic ferrofluid are shown in Fig. 5. As can be seen, the additional paramagnetic component reveals in the center of the brain spectrum in 2 h after the injection of magnetic ferrofluid into the brain. The paramagnetic component is superimposed on the Zeeman sextet of the intrinsic NP in the Mössbauer spectra measured 1 and 3 days after the injection. In a week after the injection the sextet practically disappeared and only this paramagnetic component remains in the spectra measured 7 and 28 days after the injection. This means that the injected magnetic beads, based on the synthesized $^{57}\text{Fe}_3\text{O}_4$ nanoparticles, undergo an intensive biodegradation in the live brain. Such changes in the shape of the Mössbauer spectra of the biodegradable magnetic beads have been studied in Ref. [33]. It was shown that nanosized superparamagnetic particles were combined into groups in the initial ferrofluid and were connected inside each group by magnetic dipole interaction. It was found that the appearance of a paramagnetic doublet in the spectrum of mouse liver is caused by the decrease of the magneto-dipole interaction between the superparamagnetic nanoparticles. So, in our case, the dextran coated intrinsic nanobeads disintegrated in the brain into separate superparamagnetic $^{57}\text{Fe}_3\text{O}_4$ nanoparticles during a week. Then the concentration of the resulting superparamagnetic nanoparticles in the brain monotonically falls with time.

Just in a few hours after injection, the liver spectrum (right column) demonstrated an appearance of a weak six-line component, corresponding to the initial nanobeads, and the central superparamagnetic doublet, corresponding to the separated $^{57}\text{Fe}_3\text{O}_4$ nanoparticles. Then the concentration of exogenous iron in the liver rises reaching its maximum in 3 days. With further increase in time after injection the concentration of nanoparticles in the liver begins to fall. This is illustrated in Fig. 6. In the figure the dependence of the areas of the Mössbauer spectra of the brain and liver on time after administration the ferrofluid into the ventricle of the brain is shown. In the first approximation, the areas of the spectra are proportional to the concentrations of exogenous iron in the samples of the organs.

Within the framework of this work, the authors had no intention to investigate the distribution and biodegradation of exogenous iron in the spleen of experimental animals. Initially it was assumed that the biodegradation processes in the liver and spleen are similar due to the presence in these organs large amounts of the same iron depositing protein ferritin. However, histological

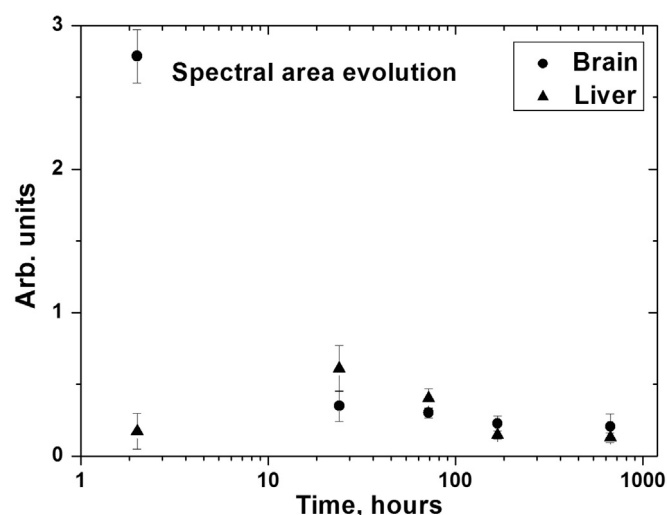


Fig. 6. Dependence of the areas of Mössbauer spectra of exogenous iron in brain and liver on time after administration the ferrofluid into the ventricle of the brain.

examination of the liver and spleen, presented in Fig. 3, showed a fundamental difference in the mechanisms of processing of iron nanoparticles in these organs. Based on these data, authors plan to conduct a more detailed study of total biodegradation processes of magnetic nanoparticles in the brain, liver and spleen in the near future.

3. Conclusion

It was found that the dextran coated magnetic nanobeads following their injection into the cerebrospinal liquid of live brain undergo an intensive disintegration into separate superparamagnetic nanoparticles in the same manner, as described before for the nanobeads after their injection into the blood [33]. The blood brain barrier does not prevent the transfer of the superparamagnetic particles from the ventricles of the brain to the liver and spleen. Therefore it can be concluded that the biodegradation of the magnetic beads, after their injection to the ventricles of brain follows the same path as that of the magnetic beads after their injection to the blood.

Acknowledgment

This work is supported in part by the Russian Science Foundation under Grant 14-15-01096.

References

- M.W. Brightman, Morphology of blood–brain interfaces, *Exp. Eye Res.* 25 (Suppl) (1977) 1–25.
- Choi, et al., Minimally invasive molecular delivery into the brain using optical modulation of vascular permeability, *Proc. Natl. Acad. Sci.* 108 (22) (2011) 9256–9261.
- W.M. Pardridge, Blood–brain barrier delivery, *Drug Discov. Today* 12 (2007) 54–61.
- A. Holtmaat, et al., Long-term, high-resolution imaging in the mouse neocortex through a chronic cranial window, *Nat. Protoc.* 4 (2009) 1128–1144.
- H.T. Xu, F. Pan, G. Yang, W.B. Gan, Choice of cranial window type for in vivo imaging affects dendritic spine turnover in the cortex, *Nat. Neurosci.* 10 (2007) 549–551.
- H. Hofmann, A. Petri, M. Chastellain, M. Hofmann, Superparamagnetic nanoparticle preparation for medical application, *Eur. Cell Mater.* 2 (2001) 29–30.
- A. Ito, M. Shinkai, H. Honda, T. Kobayashi, Medical application of functionalized magnetic nanoparticles, *J. Biosci. Bioeng.* 100 (2005) 1–11.

8. I. Safarik, M. Safarikova, Magnetic nanoparticles and biosciences, *Mon. Chem.* 133 (2002) 737–759.
9. B. Chertok, B.A. Moffat, A.E. David, et al., Iron oxide nanoparticles as a drug delivery vehicle for MRI monitored magnetic targeting of brain tumors, *Bio-materials* 29 (4) (2008) 487–496.
10. Zainulabedin M. Saiyed, Nimisha H. Gandhi, Madhavan P.N. Nair, Magnetic nanoformulation of azidothymidine 5'-triphosphate for targeted delivery across the blood–brain barrier, *Int. J. Nanomed.* 5 (2010) 157–166.
11. C. Riviere, M.S. Martina, C. Riviere, et al., Magnetizing targeting of nanometric magnetic fluid loaded liposomes to specific brain intravascular areas: a dynamic imaging study in mice, *Radiology* 244 (2007) 439–448.
12. H. Dou, C.B. Grotepas, J.M. McMillan, et al., Macrophage delivery of nanoformulated antiretroviral drug to the brain in a murine model of NeuroAIDS, *J. Immunol.* 183 (2009) 661–669.
13. H. Dou, C.J. Destache, J.R. Morehead, et al., Development of a macrophagebased nanoparticle platform for antiretroviral drug delivery, *Blood* 108 (2006) 2827–2835.
14. V.H. Perry, D.C. Anthony, S.J. Bolton, H.C. Brown, The blood–brain barrier and inflammatory response, *Mol. Med.* 3 (1997) 335–341.
15. S. Jain, V. Mishra, P. Singh, P.K. Dubey, D.K. Saraf, S.P. Vyas, RGD-anchored magnetic liposomes for monocytes/neutrophils-mediated brain targeting, *Int. J. Pharm.* 261 (2003) 43–55.
16. Liu, et al., Magnetic resonance monitoring of focused ultrasound/magnetic nanoparticle targeting delivery of therapeutic agents to the brain, *Proc. Natl. Acad. Sci.* 107 (34) (2010) 15205–15210, www.pnas.org/cgi/doi/10.1073/pnas.1003388107.
17. N. McDannold, N. Vykhodtseva, K. Hynynen, Blood–brain barrier disruption induced by focused ultrasound and circulating preformed microbubbles appears to be characterized by the mechanical index, *Ultrasound Med. Biol.* 34 (2008) 834–840.
18. D.M. Polikarpov, R.R. Gabbasov, V.M. Cherepanov, M.A. Chuev, V.A. Korshunov, M.P. Nikitin, S.M. Deyev, V.Y. Panchenko, Biodegradation of magnetic nanoparticles in rat brain studied by Mössbauer spectroscopy, *IEEE Trans. Magn.* 49 (2013) 436–439.
19. L.L. Muldoon, M. Sandor, K.E. Pinkston, E.A. Neuwelt, Imaging, distribution, and toxicity of superparamagnetic iron oxide magnetic resonance nanoparticles in the rat brain and intracerebral tumor, *Neurosurgery* vol. 57 (2005) 785–796.
20. D. Polikarpov, V. Cherepanov, M. Chuev, R. Gabbasov, I. Mischenko, M. Nikitin, Y. Vereshagin, A. Yurenia, V. Panchenko, Mössbauer evidence of $57\text{Fe}_3\text{O}_4$ based ferrofluid biodegradation in the brain, *Hyperfine Interact.* 226 (2014) 421–430.
21. G. Paxinos, C. Watson, *The Rat Brain in Stereotaxic Coordinates*, Academic, New York, 1998.
22. J.L. Kirschvink, A. Kobayashi-Kirschvink, B.J. Woodford, Magnetite biomineralization in the human brain, *Proc. Natl. Acad. Sci.* 89 (1992) 7683–7687.
23. J.R. Dunn, M. Fuller, J. Zoeger, J. Dobson, F. Heller, J. Hammann, E. Caine, B. M. Moskowitz, Magnetic material in the human hippocampus, *Brain Res. Bull.* 36 (1995) 149–153.
24. J. Dobson, P. Grassi, Magnetic properties of human hippocampal tissue: Evaluation of artefact and contamination sources, *Brain Res. Bull.* 39 (1996) 255–259.
25. C. Quintana, M. Lancin, C. Marchic, M. Pe´rez, J. Martin-Benito, J. Avila, J. L. Carrascosa, Initial studies with high resolution TEM and electron energy loss spectroscopy studies of ferritin cores extracted from brains of patients with progressive supranuclear palsy and Alzheimer disease, *Cell Mol. Biol.* 46 (2000) 807–820.
26. C. Quintana, J.M. Cowley, C. Marhic, Electron nanodiffraction and high-resolution electron microscopy studies of the structural and composition of physiological and pathological ferritin, *J. Struct. Biol.* 147 (2004) 166–178.
27. D. Hautot, Q.A. Pankhurst, N. Khan, J. Dobson, Preliminary evaluation of nanoscale biogenic magnetite in Alzheimer's disease brain tissue, *Proc. R. Soc. Lond. Ser. B* 270 (2003) S62–S64.
28. F. Brem, A.M. Hirt, M. Winkelhofer, K. Frei, Y. Yonekawa, H.G. Wieser, J. Dobson, Magnetic iron compounds in the human brain: a comparison of tumour and hippocampal tissue, *J. R. Soc. Interface* 3 (11) (2006) 833–841.
29. H. Spatz, On the visualization of iron in the brain, especially in the centers of the extrapyramidal motor system, *Z. Ges. Neurol. Psychiatr.* 77 (1922) 261–390.
30. E.M. Haacke, N.Y. Cheng, M.J. House, et al., Imaging iron stores in the brain using magnetic resonance imaging, *Magn. Reson. Imaging* 23 (2005) 1–25.
31. P. Lieu, M. Heiskala, P.A. Peterson, Y. Yang, The roles of iron in health and disease, *Mol. Asp. Med.* 22 (2001) 1–87.
32. M. Nikitin, R. Gabbasov, V. Cherepanov, M. Chuev, M. Polikarpov, V. Panchenko, S. Deyev, Magnetic nanoparticle degradation in vivo studied by Mössbauer spectroscopy, *Proc. Am. Inst. Phys. Conf. Ser.* vol. 1311 (2010) 401–407.
33. R.R. Gabbasov, V.M. Cherepanov, M.A. Chuev, M.A. Polikarpov, V.Y. Panchenko, Study of interparticle interaction in conjugates of magnetic nanoparticles injected into mice, *Hyperfine Interact.* (206) (2012) 71–74.